OCEAN OXYGEN

Large-scale ocean deoxygenation during the Paleocene-Eocene Thermal Maximum

Weiqi Yao[1]*, Adina Paytan[2], Ulrich G. Wortmann[1]

The consequences of global warming for fisheries are not well understood, but the geological record demonstrates that carbon cycle perturbations are frequently associated with ocean deoxygenation. Of particular interest is the Paleocene-Eocene Thermal Maximum (PETM), where the carbon dioxide input into the atmosphere was similar to the IPCC RCP8.5 emission scenario. Here we present sulfur-isotope data that record a positive 1 per mil excursion during the PETM. Modeling suggests that large parts of the ocean must have become sulfidic. The toxicity of hydrogen sulfide will render two of the largest and least explored ecosystems on Earth, the mesopelagic and bathypelagic zones, uninhabitable by multicellular organisms. This will affect many marine species whose ecozones stretch into the deep ocean.

The geological record contains many examples in which the Earth system was out of equilibrium and large parts of the ocean were inhospitable to life. However, only few of these events can provide insight into the effects of modern fossil fuel burning. This is because either the boundary conditions are substantially different (e.g., the plate-tectonic configuration) or the rate of change is not comparable. The short-lived Paleocene-Eocene Thermal Maximum (PETM) event [~55 million years ago] (*1*) is a notable exception. Current data suggest that in the PETM, the atmosphere had to accommodate about 2500 to 4500 Gt of carbon released within 4000 years (*2*). This is an increase of the same order of magnitude as the IPCC RCP8.5 emission scenario, which projects a cumulative anthropogenic CO_2 release of 2000 GtC by 2100 (*3*). Although the carbon dioxide release rate during the PETM was about a factor of 10 slower, it is our best analog for studying nonlinear feedbacks and consequences of the anthropogenic carbon cycle perturbation.

The geochemical cycles of carbon and sulfur are linked through microbial sulfate reduction (MSR), where the electron transfer from sulfate to sulfide provides the energy to respire organic matter (OM) back to CO_2. Combined, these cycles constitute the dominant control on atmospheric oxygen (*4*, *5*). Owing to their drastically different residence times (0.1 versus 10 million years) (*4*), they are rarely considered together. Our data suggest, however, that MSR can alter the redox state of the marine sulfur reservoir on time scales that are comparable to that of the carbon cycle. This has three important implications: (i) Unlike oxic respiration, MSR also produces H_2S, which is toxic to most life forms even at low concentrations; (ii) if we accept the premise that the PETM is a model for the present-day oceans, the time scales of the observed changes in the redox state of marine sulfur suggest that similar processes could affect the oceans in the near future; (iii) the development of oxygen-free waters creates a sizable but intermittent reservoir in the global sulfur cycle, with fluxes exceeding traditional weathering and burial flux estimates.

The mass and sulfur-isotope ratio of seawater sulfate are controlled by sulfur delivered to the oceans via weathering and volcanic degassing and sulfur removed from the oceans via burial of sulfur-bearing minerals. In marine sediments, sulfur is present in its oxidized form as sulfate-bearing evaporite salts and in its reduced state as metal sulfides. Sulfate-bearing evaporites precipitate with little or no fractionation relative to seawater, and thus have a limited effect on the S-isotope ratio of seawater sulfate (*5*, *6*). By contrast, MSR has a preference for ^{32}S, and thus exerts a substantial influence on the seawater $^{34}S/^{32}S$ ratio (*7*, *8*). In this study, we use pristine authigenic marine barite crystals to trace the evolution of the marine S-isotope ratio across the PETM. We report our results in the traditional delta notation ($\delta^{34}S$), which expresses the isotopic ratio of $^{34}S/^{32}S$ as a difference relative to a reference standard:

$$\delta^{34}S = \frac{\left(\frac{^{34}S}{^{32}S}\right)_{Sample} - \left(\frac{^{34}S}{^{32}S}\right)_{Standard}}{\left(\frac{^{34}S}{^{32}S}\right)_{Standard}} \times 1000[‰]$$

where ^{X}S denotes the concentration of the respective sulfur isotope. All results are reported relative to the Vienna Canyon Diabolo Troillite (VCDT).

We observe a 1‰ shift in $\delta^{34}S$ during the PETM (Fig. 1), which implies the removal of 8×10^{16} mol of reduced sulfur within 50 thousand years from the oceans (assuming a marine sulfate concentration of 5 mM) (*9*). This requires more than double the pre-PETM steady-state pyrite burial flux. More important, the rapid decay of the S-isotope excursion occurs within ~100 thousand years. Owing to the large size of the marine sulfate reservoir and the small input and output fluxes to the ocean, the marine S-isotope ratio is expected to retain the peak S-isotope values of the excursion for millions of years before returning to pre-excursion conditions. The observed rapid decay of the S-isotope excursion requires the input of 8×10^{16} mol of isotopically light sulfur back into the ocean before the end of the PETM.

Changes in pyrite burial are traditionally invoked to explain changes in seawater $\delta^{34}S$. It is assumed that most of the pyrite burial happens on continental shelves (*10*, *11*). As such, pyrite burial rates correlate with sea-level variations, i.e., during high stands, shelf areas expand and pyrite burial increases, whereas during low stands, shelf areas contract and previously buried pyrite is reoxidized (*11*). Sea-level estimates suggest a rise

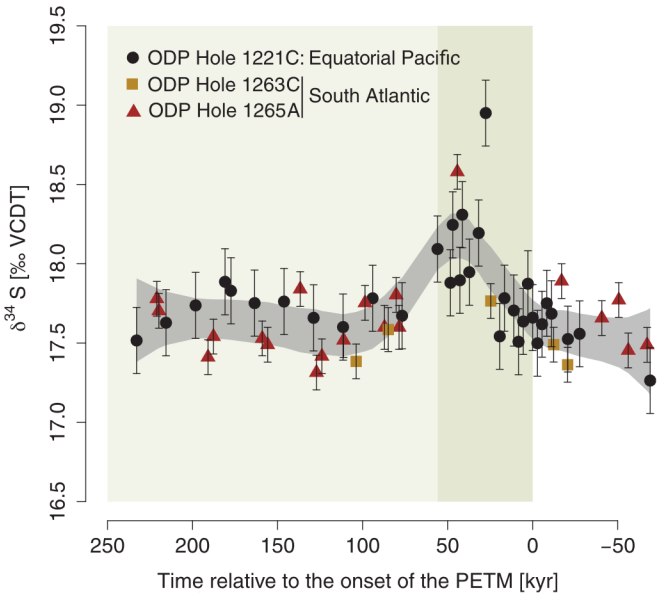

Fig. 1. $\delta^{34}S$ data of authigenic marine barite crystals across the PETM. The gray envelope denotes the 95% confidence interval of the LOESS regression (see supplementary materials). Shaded boxes indicate the extents of the main and total PETM interval (*1*). Error bars are 1σ.

[1]Department of Earth Sciences, University of Toronto, Toronto, Ontario, M5S 3B1, Canada. [2]Institute of Marine Science, University of California–Santa Cruz, Santa Cruz, CA 95064, USA.
*Corresponding author. Email: weiqi.yao@mail.utoronto.ca

on the order of 25 m during the PETM (*12*). Using previously published parametrizations (*11*), this increase results in the additional burial of 4.45×10^{10} mol pyrite per year, about 4% of that required to explain the observed isotope shift. The idea that the shelf acts as a transient pyrite reservoir has been expressed previously (*11*, *13*), but the observed isotope signal requires an increase in the global shelf area equivalent to 13 to 32 times the size of the contiguous United States. Clearly, these numbers depend on a variety of assumptions, chiefly, the OM and pyrite burial rates on the shelves; however, they do demonstrate the magnitude of required flux changes.

Previous authors proposed that the importance of continental shelves for pyrite burial may have been overstated (*11*, *14*) and that the long-term burial of pyrite is controlled by the intensity of anaerobic methane oxidation (AMO) on continental slopes (*14*). This idea is particularly intriguing because it links pyrite burial to subseafloor methane flux, which in turn has been suggested as a possible explanation for the negative carbon-isotope excursion in the PETM (*14*, *15*). In this scenario, the rapid release of isotopically light methane would not only drive the observed C-cycle excursion but also increase pyrite burial rates.

Linking pyrite burial flux to methane flux is elegant and provides a plausible explanation for the rise in the marine $\delta^{34}S$ ratio during the PETM. Furthermore, once the methane has been vented, gas hydrate reservoirs will have to recharge and thus AMO fluxes and AMO-associated pyrite burial rates will cease (*14*). However, even if we assume the extreme case that all pyrite burial is AMO-controlled, it would take at least 0.2 million years to return the marine $\delta^{34}S$ ratio back to its pre-excursion value (see supplementary materials). That means it is not sufficient just to inhibit all pyrite burial; rather, we need to inject large quantities of isotopically light S into the oceans to explain the observed S-isotope signal. The speed and magnitude of the required ^{32}S flux require a transient reservoir of ^{32}S-enriched sulfur that is sufficiently large to hold 8×10^{16} mol of isotopically depleted S and can be charged and released in less than 100 thousand years.

Here we propose that the marine oxygen minimum zone (OMZ) constitutes such a reservoir. With the exception of a few upwelling zones, oxygen concentrations in the OMZ are usually high enough to render MSR energetically unfavorable. However, the marine oxygen pool is small, and changes in circulation or export production can alter the oxygen content of the OMZ rapidly. Once oxygen concentrations in the OMZ drop below 4 μM (*16*), MSR becomes the dominant OM remineralization pathway. In the modern ocean, MSR is limited by OM supply and the diffusive supply of sulfate into the sediment column. Shifting the location of sulfate reduction from the sediment into the intermediate water column would not only increase the availability of sulfate, but drastically increase the quality and quantity of OM. This will accelerate the globally integrated sulfate reduction flux and transfer ^{32}S into the OMZ, effectively separating the ocean into two sulfur reservoirs.

To estimate the required changes to the OMZ, we use S-isotope fractionation factors (α) between 43 and 70‰ (*7*, *8*), and an average sulfide concentration up to 0.5 mM, well below the 1 mM threshold where chemocline upwelling and the subsequent release of H_2S into the atmosphere become a possibility (*17*). The value of 0.5 mM is high compared to sulfide concentrations observed in anoxic upwelling zones in the modern ocean (*16*), but well within the limits of marine sulfide concentrations observed within more restricted settings (e.g., 6.14 mM in Framvaren Fjord) (*18*). Modeling the data using the statistically significant maximum of 18.35‰ (Fig. 2) requires sulfidic water volumes between 1.6×10^{17} to 2.6×10^{17} m^3. The highest measured $\delta^{34}S$ value (18.95‰) can be explained with a sulfidic water volume of no more than 2.7×10^{17} m^3 for α of 70‰. To put these estimates into perspective: In the modern ocean, the OMZ sensu stricto (O_2 < 20 μM) encompasses about 1% of the global ocean volume (1.38×10^{18} m^3) (*19*), whereas the above numbers suggest an order-of-magnitude increase to 10 to 20% of the ocean volume. Indeed, several studies suggest that low O_2 or anoxic waters were present during the PETM at intermediate depths in many ocean basins (*20*–*23*).

Modeling predictions exploring the effects of anthropogenic climate change suggest that measurable oxygen loss from the subarctic North Pacific will occur by 2030 to 2040 (*24*) and that the total volume of suboxic ocean water will

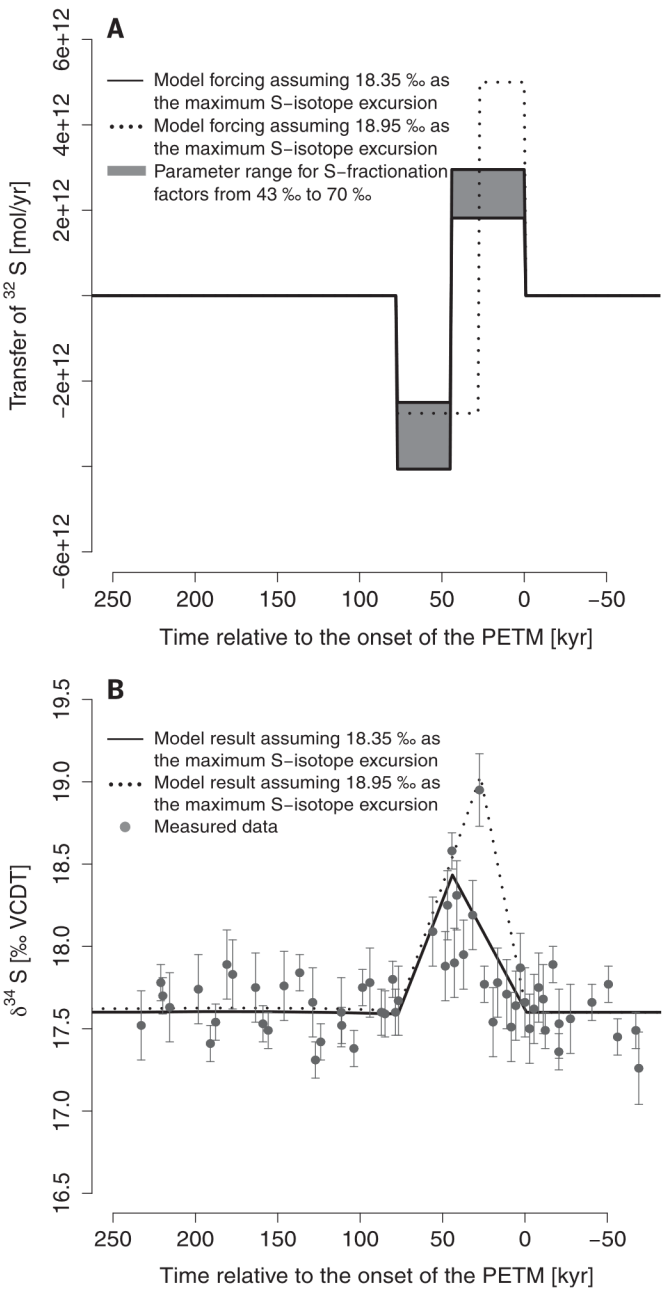

Fig. 2. Model forcing and the resulting S-isotope ratios versus measured data. (**A**) Transfer of ^{32}S into and out of the OMZ. (**B**) Resulting changes in the marine sulfate $\delta^{34}S$ across the PETM. See supplementary materials for full model results. Note that in order to model the peak at 18.95‰, the timing of the flux changes has to be adjusted.

expand by 50% by 2100 (*25*). Once local oxygen concentrations drop below 4 μM (*16*), sulfate reduction will commence, resulting in the production of H_2S, which is toxic at levels as low as 4 μg/liter (*26*). This will (A) create an ocean internal reservoir of reduced sulfur; (B) create an ocean that is no longer well mixed with respect to sulfate; and (C) compress the ecozones of fish species that venture in the mesopelagic and bathypelagic zones (*27*) and change their ecosystem structure, which could jeopardize 10 to 50% of worldwide pelagic predator diversity (*27*) with unknown consequences for global fish stocks. Our findings suggest that (A) and (B) have been well expressed during the PETM, and given the similarities between the PETM and the IPCC RCP8.5 emission scenario, (C) will be a possibility in the not-too-distant future.

REFERENCES AND NOTES

1. F. Nunes, R. Norris, in *Proceedings of the Ocean Drilling Program, Scientific Results*, P. Wilson, M. Lyle, J. Firth, Eds. (College Station, TX, 2005), vol. 199, pp. 1–12.
2. R. Zeebe, A. Ridgwell, J. Zachos, *Nat. Geosci.* **9**, 325–329 (2016).
3. "IPCC, *Climate Change 2013: The Physical Science Basis. Contribution of Working Group I to the Fifth Assessment Report of the Intergovernmental Panel on Climate Change*, T. F. Stocker *et al*., Eds. (Cambridge Univ. Press, 2013).
4. J. C. Walker, *Mar. Geol.* **70**, 159–174 (1986).
5. U. G. Wortmann, B. M. Chernyavsky, *Nature* **446**, 654–656 (2007).
6. G. Claypool, W. Holser, I. Kaplan, H. Sakai, I. Zak, *Chem. Geol.* **28**, 199–260 (1980).
7. I. Kaplan, K. Emery, S. Rittenberg, *Geochim. Cosmochim. Acta* **27**, 297–331 (1963).
8. U. Wortmann, S. Bernasconi, M. Böttcher, *Geology* **29**, 647–650 (2001).
9. U. G. Wortmann, A. Paytan, *Science* **337**, 334–336 (2012).
10. A. Turchyn, D. Schrag, *Earth Planet. Sci. Lett.* **241**, 763–779 (2006).
11. S. Markovic, A. Paytan, U. Wortmann, *Biogeosciences* **12**, 3043–3060 (2015).
12. K. G. Miller *et al*., *Science* **310**, 1293–1298 (2005).
13. J. Higgins, D. Schrag, *Earth Planet. Sci. Lett.* **245**, 523–537 (2006).
14. G. Dickens, *Clim. Past* **7**, 831–846 (2011).
15. G. Dickens, J. O'Neil, D. Rea, R. Owen, *Paleoceanography* **10**, 965–971 (1995).
16. V. Brüchert *et al*., *Geochim. Cosmochim. Acta* **67**, 4505–4518 (2003).
17. L. Kump, A. Pavlov, M. Arthur, *Geology* **33**, 397–400 (2005).
18. W. Landing, S. Westerlund, *Mar. Chem.* **23**, 329–343 (1988).
19. A. Paulmier, D. Ruiz-Pino, *Prog. Oceanogr.* **80**, 113–128 (2009).
20. M. Nicolo, G. Dickens, C. Hollis, *Paleoceanography* **25**, PA4210 (2010).
21. A. Dickson, A. Cohen, A. Coe, *Geology* **40**, 639–642 (2012).
22. A. Winguth, E. Thomas, C. Winguth, *Geology* **40**, 263–266 (2012).
23. X. Zhou *et al*., *Paleoceanography* **31**, 1532–1546 (2016).
24. M. C. Long, C. Deutsch, T. Ito, *Global Biogeochem. Cycles* **30**, 381–397 (2016).
25. A. Oschlies, K. Schulz, U. Riebesell, A. Schmittner, *Global Biogeochem. Cycles* **22**, GB4008 (2008).
26. L. Smith, D. Oseid, I. Adelman, S. Broderius, Effect of hydrogen sulfide on fish and invertebrates. Part I – Acute and chronic toxicity studies. *Ecol. Res. Tech. Rep. Ser. No.3* (U.S. Environmental Protection Agency, 1976).
27. L. Stramma *et al*., *Nat. Clim. Chang.* **2**, 33–37 (2012).

ACKNOWLEDGMENTS

We thank G.R. Dickens and S. Markovic for discussions and comments on an early draft of this paper; H. Li for support with the isotope analysis; and the three anonymous reviewers for helping to improve this manuscript. **Funding:** This research was supported by a Discovery Grant of the Natural Sciences and Engineering Research Council of Canada (NSERC) to U.G.W. and a National Science Foundation (NSF) CAREER grant OCE-0449732 to A.P. **Author contributions:** All authors contributed to the ideas expressed in this manuscript. W.Y. and U.G.W. developed the project. A.P. provided barite samples. W.Y. performed isotope measurements, data analysis, and computations and did the art work. W.Y., U.G.W., and A.P. were responsible for data interpretation and manuscript writing. **Competing interests:** The authors declare no competing interest. **Data and materials availability:** All data are available in supplementary materials.

SUPPLEMENTARY MATERIALS

www.sciencemag.org/content/361/6404/804/suppl/DC1
Materials and Methods
Figs. S1 to S8
Tables S1 and S2
References (*28*–*58*)

27 December 2017; accepted 7 July 2018
Published online 19 July 2018
10.1126/science.aar8658